Scaling of Efficiency with Applied Magnetic Field in Magnetoplasmadynamic Thrusters

Dan Lev[*] and Edgar Y. Choueiri [†]

Electric Propulsion and Plasma Dynamics Laboratory (EPPDyL)

Princeton University, Princeton, NJ, 08544, USA

An investigation of the scaling of thrust efficiency with the applied magnetic field in applied-field magnetoplasmadynamic thrusters (AF-MPDTs) is carried out in order to provide guidelines for scaling and controlling AF-MDPT performance. Thruster voltage measurements were made at different current, applied magnetic field and mass flow rate levels in a 30 kW lithium-fed AF-MPDT. The efficiency was then calculated using the voltage data along with a semi-empirical thrust formula derived and verified previously for the same thruster. The non-useful voltage component (the voltage associated with the thruster's power losses) was found to scale linearly with current and applied magnetic field and inversely with mass flow rate. This behavior was attributed to electrode sheath effects and decreased conductivity with increasing applied magnetic field. The efficiency was found to increase with applied magnetic field for all current and mass flow rate values and the enhancement of the efficiency by the applied magnetic field was found to be greater when the mass flow rate is reduced. The observed minimum in the efficiency vs current curve was related to interplay between the components of the thrust and was shown experimentally and analytically to increase with increasing applied field and decreasing mass flow rate.

Nomenclature

η Efficiency
J Total applied current, A
B Applied magnetic field, T
T Thrust, N
V Voltage, V
P Power, kW
$\dot{m}$ Mass flow rate, mg/s
r Radius
u_e Exhaust velocity, m/s

Subscript
c Cathode
a Anode
emf Electro-motive force
E Electrodes
res Resistive

---

[*]Graduate Research Assistant, EPPDyL; Student Member, AIAA.

[†]Chief Scientist, EPPDyL; Professor, Applied Physics Group, Mechanical and Aerospace Engineering Department; Fellow AIAA.

American Institute of Aeronautics and Astronautics

I. Introduction

Magnetoplasmadynamic thrusters (MPDTs) are a subclass of plasma thrusters with an overwhelmingly electromagnetic acceleration mechanism involving the interaction of a current between an anode and a cathode and a magnetic field which could be applied or induced by the current itself. This interaction gives rise to a Lorentz force density ($f = j \times B$) that accelerates propellant downstream and out of the thruster. The thrust generation mechanism of the self-field MPDT is well understood and was characterized by Maecker[1] and Jahn[2] and analyzed by Choueiri.[3] High thrust and thrust density are also the big advantages that MPDTs have over other types of electric propulsion devices, such as the Hall thruster or the ion thruster. MPDTs promise a wide range of thrust levels (100 mN - 100 N) that depends on the power level, along with high specific impulse (1000-5000 s) a high thrust efficiency, ($10-25\%$ with argon and up to 60% with lithium propellant), and the ability to process 100's of kW in a single compact device.

It has been well established that the addition of an applied magnetic field to the thruster increases its performance significantly. This is often necessary at low power levels (below 100 kW) where the current is too low for the self-induced magnetic field to be sufficient. Thrust, efficiency and specific impulse tend to increase with the applied magnetic field intensity. It has been observed[4] that the thrust increases linearly with the product JB, where J is the total current applied to the thruster and B is the value of the applied magnetic field measured at the solenoid's center. The detailed physics behind the acceleration mechanism in applied magnetic field MPDT (AF-MPDT) is not yet fully understood and further experimental research is needed.

The focus of ongoing studies on AF-MPDTs is on the most promising variant called the **Li**thium **L**orentz **F**orce **A**ccelerator (LiLFA). The LiLFA is a steady state AF-MPDT that uses lithium as a propellant and a multi-channel hollow cathode. Lithium has great potential for two main reasons: 1) Lithium's first ionization potential (5.4 eV) is significantly lower than that of other, commonly-used propellants such as argon (15.7 eV), xenon (12.1 eV) or hydrogen (13.6 eV), while lithium's second ionization potential is significantly higher than that of these propellants. Therefore the frozen flow losses are lower in lithium-fed MPDTs. 2) Lithium (especially with the addition of small amounts of barium) lowers the work function of the thruster's cathode, thus enabling cathode operation at much lower temperatures[5] and reducing cathode erosion. The above two advantages make lithium a very good candidate for high power AF-MPDTs. Lithium-fed MPDTs have high efficiencies, in the range of 20% to 60% depending on the power level, and due to their low electrode erosion rate, have demonstrated hundreds of hours of high-power operation (0.5 MW) without showing significant damage.[6]

The voltage-current, $V-J$, characteristics of the MPDT are important in evaluating the scaling of thrust efficiency in different operating regimes because efficiency is calculated using the power required to operate the thruster, which is equal to the product VJ. Changing the applied current, mass flow rate, or applied magnetic field affects such plasma properties as the plasma resistivity and exhaust velocity. This in turn changes the required voltage to sustain operation and the generated thrust, leading to variations in efficiency for different operational regimes.

Previously voltage models were sought in order to determine how the thruster's efficiency changes with operation and thruster parameters. Tikhonov[7] suggested a semi-empirical voltage model that is difficult to implement as it requires experimental measurements of the electrodes' sheaths and knowledge of the electron temperature. Mikellides and Turchi[8] suggested and verified another analytical model but the experimental data with which it agrees spans a narrow spectrum of voltage-current behavior.

In this study, we perform a qualitative and experimental investigation of the voltage-current and efficiency-current characteristics in the LiLFA with the aim of shedding more light on the various regimes in these characteristics. First, we measure the voltage of the LiLFA for different current, applied magnetic field and mass flow rate values. We then use a mathematical expression for thrust derived by Tikhonov[9] and based on previous experimental study performed on the LiLFA in order to calculate the thrust efficiency. The observed trends of the efficiency with current, applied magnetic field and mass flow rate are then analyzed after which a thorough physical interpretation is given to explain the observations.

American Institute of Aeronautics and Astronautics

II.   Experimental Setup

A.   Steady State Low Power Facility

All experiments were performed in the Steady State Low Power (SSLP) facility at the Electric Propulsion and Plasma Dynamics Lab (EPPDyL) at Princeton University. The SSLP facility consists of a large cylindrical vacuum chamber, 1.5 m in diameter and 3.6 m long, made of stainless steel in order to withstand high temperatures. An active cooling jacket uses chilled water to maintain a moderate temperature along the chamber's inner walls. The ultimate vacuum of this system is 1.7×10^{-5} Torr (2.266×10^{-3} Pa) and is obtained using a 1.22 m CVC Type PMC-48C (95,000 l/s) diffusion pump, a Leybold Vacuum Products Inc. RUVAC WSU-2000 1342 CFM (630 l/s) Roots accelerator, and a 150 CFM (71 l/s) Stokes Microvac mechanical pump with which it is placed in series. Low pressure is easily kept during thruster operation since lithium is solid at room temperature and therefore condenses on the inner walls of the vacuum chamber.

An ingot of about 150 g of lithium is loaded into a small stainless steel reservoir, 80 mm in diameter and 166 mm in length. We perform the loading of the reservoir under argon atmosphere in a glove box in order to keep the lithium in an inert environment. The reservoir is then attached to the thruster feeding system (Fig. 1) in the vacuum chamber, which is then closed and pumped down while a steady flow of argon in the reservoir keeps the lithium from reacting with air.
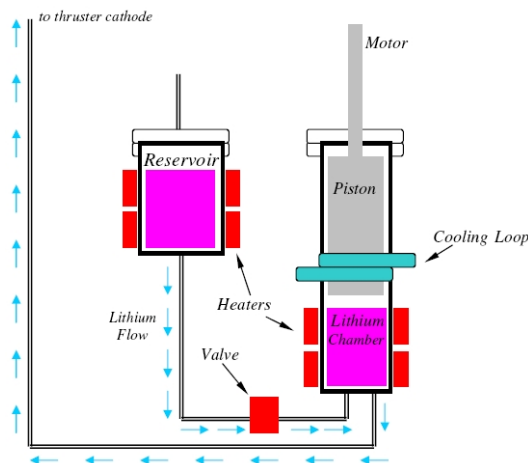

Figure 1. LiLFA Lithium Feed System. Lithium flows from the reservoir to the cylinder where it is pushed by the piston through the pipe line and into the thruster cathode

The lithium is fed through a dedicated feed system that is located in the vacuum chamber and which whose design and calibration were discussed by Kodys et. al.[10] Once brought to its melting temperature, lithium flows out of the reservoir and into a cylinder where it awaits ejection by a piston whose position is carefully controlled. Once forced out of the cylinder, liquid lithium flows through a stainless steel pipe $1/4''$ in diameter to the thruster's cathode where it is vaporized by a heater inside the cathode. The entire feed system requires about 1 kW of electric power and is controlled by four variacs to maintain a temperature of about 250°C during steady-state operation, about 70°C above lithium's melting temperature.

The lithium mass flow rate is directly proportional to the piston's velocity inside the cylinder,[10] and can be varied within a range of 1-200 mg/s. Operation of the thruster itself is accomplished using a 'Miller' SRS-1000 30 kW generator capable of supplying DC current up to 1500 A.

B.   The Thruster

The LiLFA (Fig. 2) was built and initially tested at **M**oscow **A**viation **I**nstitute (MAI). It was transferred to Princeton's EPPDyL in 1998. It consists of a conical anode made of tungsten with an upstream inner diameter of 45 mm and a downstream inner diameter of 70 mm. The cylindrical multi-channel hollow cathode (MCHC), also made of tungsten, has an inner diameter of 19.2 mm and a length of 215 mm (100 mm in the thruster cavity). Its tip consists of 68 small rods, each 2 mm in diameter and 14 mm in length. The cathode

American Institute of Aeronautics and Astronautics

evaporates the incoming liquid lithium provided by the feed system due to its high temperature of well over 1000°C, maintained by a graphite heater requiring approximately 1.2 kW of power.

During operation the cathode reaches temperatures of over 2000°C[11] while the anode reaches temperatures of up to 1500°C.

The applied magnetic field is generated by a water cooled solenoid, 280 mm in outer diameter and 120 mm in inner diameter. The solenoid consists of a copper tube 8 mm in diameter which is turned 56 times in order to generate magnetic field values up to 0.08 T with current of 250 A. At this operational point the solenoid requires approximately 2.6 kW of power.
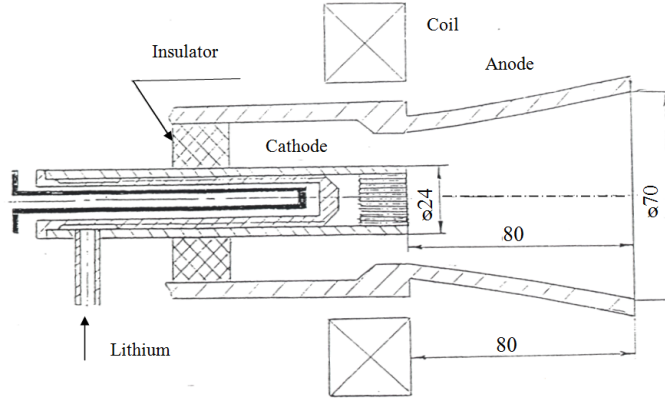

Figure 2. Cross-sectional view of the Lithium Lorentz Force Accelerator (All dimensions are in millimeters)

C. Voltage and Current Measurements

Total thruster voltage was measured across the anode and cathode through a voltage divider that matches the impedance of the data acquisition system. The total thruster current was measured using a Bell Sensor (type IF-5020P Series) measuring the current on the anode line.

D. Experimental Conditions

All measurements mentioned above were taken at three different mass flow rates, 5 mg/s, 8 mg/s and 20 mg/s. For each of the three mass flow rates measurements were taken for applied magnetic field values between 0 T and 0.08 T, and total thruster current values between approximately 100 A and 800 A and within the limits of the power supply. A total of 14 different cases with and without applied magnetic field were studied. (All magnetic field values were measured at the center of the solenoid).

III. Experimental Observations

In order to estimate the thruster's efficiency both the total power and the thrust power are required as seen in the expression

$$\eta = \frac{P_{acc}}{P_{tot}} = \frac{\dot{m}u_e^2}{2P_{tot}} = \frac{T^2}{2J\dot{m}V_{tot}}, \tag{1}$$

where V_{tot} is the total voltage and $V_{emf} = T^2/(2J\dot{m})$ is the back electromotive voltage. Therefore, aside from measuring the current, mass flow rate and voltage, a knowledge of the scaling of thrust with current is needed in order to calculate the sought $\eta - J$ scaling.

For that we employ a semi-empirical thrust model derived and verified experimentally by Tikhonov.[7] Tikhonov's thrust relation, shown below, was formulated based on experimental study conducted on the 30 kW LiLFA and higher power versions of it (> 100 kW)[12][13],[14]

$$T(J) = 1.71 \times 10^{-7}J^2 + (0.1B_a 2r_a)J + 1.6\dot{m}a_0. \tag{2}$$

American Institute of Aeronautics and Astronautics

Here B_a is the applied magnetic field at the anode face ($B_a = B_c/2$ in the LiLFA) and a_0 is the sonic speed at the cathode exit. For the sonic speed we take $a_0 = \sqrt{k(\gamma_e T_e + \gamma_i T_i)/m_i}$ with the electron and ion temperatures equal 1.5 eV at the cathode exit as was measured by Tikhonov using probes. We also assume that the specific heat ratio is taken to be that of a monatomic gas ($\gamma = 5/3$). The sonic speed is therefore $a_0 = 8.3 \times 10^3$ m/s.

In Eq. 2, the first term represents the self-field component of thrust, the second term represents the applied-field component (which scales as the product JB_a), and the third term represents the gas dynamic contribution.

We note that the AF-MPDT is designed to operate at current regimes in which the self induced magnetic field generates thrust values negligible compared to the applied field and gas dynamic thrust components. The thrust formula used here was verified by comparing it to experimental data taken at MAI on the 30 kW LiLFA (Fig. 3). It can be seen that the thrust model fits the experimental data well and can be used to
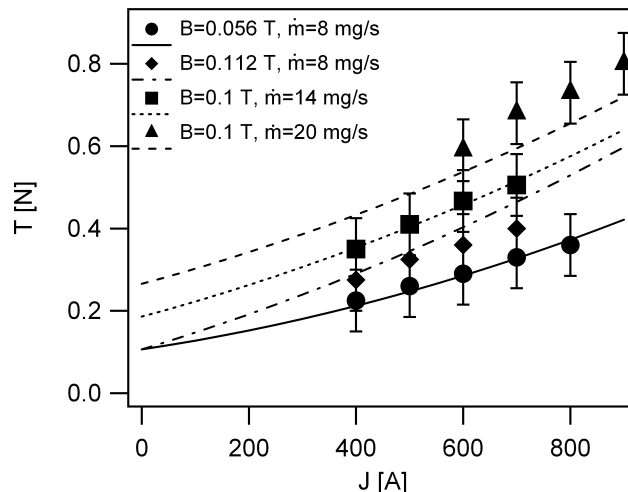

Figure 3. Thrust measurements taken at MAI on the 30 kW LiLFA along with Tikhonov's semi-empirical model.

estimate the thrust generated by the 30 kW LiLFA at different operating conditions. It should be noted that the experimental data are limited to current values higher than 400 A thus any analysis conducted at lower current values should be regarded with caution.

In Fig. 4-6 we present the voltage-current characteristics obtained for various applied magnetic field and mass flow rate values. In Fig. 7 we present the corresponding efficiencies calculated according to Eq. 1.

In Fig. 4-6 the sources of errors are due to small fluctuations in the measured voltage. Although the arc was stable during thruster operation small fluctuations in the order of 1 V were observed in most cases. In addition, we observed that for operation at higher current values the range of voltage fluctuations was larger.

It can be observed from the figures that for all cases presented both the voltage and efficiency increase with increasing magnetic field. For the case of $\dot{m} = 5$ mg/s the efficiency increases by as much as 150% from $\eta = 10\%$ to $\eta = 25\%$ at $J = 600$ A. This increase in efficiency is higher for low mass flow rate values, i.e. the lower the mass flow rate the greater the increase of efficiency with the applied field.

The mass flow rate also affects the slope of the voltage-current curves. The lower the mass flow rate the greater the slope. The voltage-current curves at $\dot{m} = 20$ mg/s seem flatter than at $\dot{m} = 5$ mg/s. We can therefore conclude that the efficiency and total voltage are more sensitive to changes in current and applied magnetic field at low mass flow rate values.

It can also be observed that for all cases presented both the voltage and efficiency have a decreasing-increasing trends with increasing current. Therefore each curve is characterized by a minimum point. Moreover, the minimum point moves to lower current values with an increasing applied field while moving to higher current values with increasing mass flow rate.
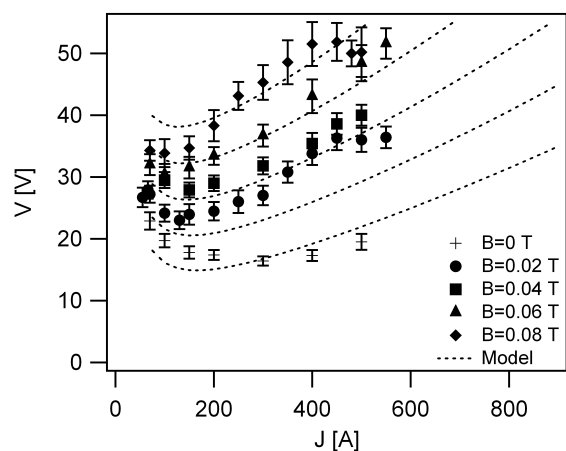
The observed trends are summarized in Table 1.

American Institute of Aeronautics and Astronautics

Figure 4. Voltage-Current characteristics for $\dot{m}$=5 mg/s. The dashed lines represent the semi-empirical voltage model presented in Eq. 4.
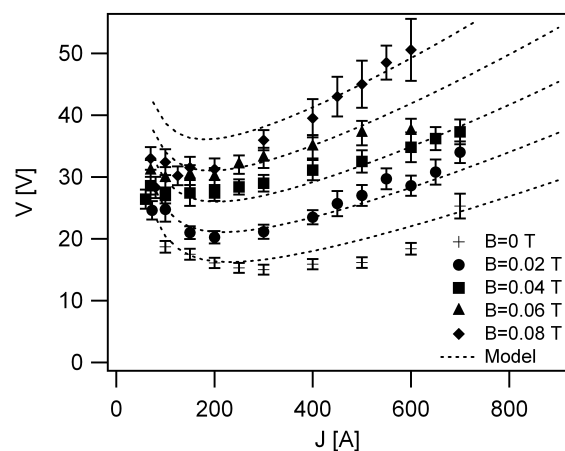

Figure 5. Voltage-Current characteristics for $\dot{m}$=8 mg/s. The dashed lines represent the semi-empirical voltage model presented in Eq. 4.
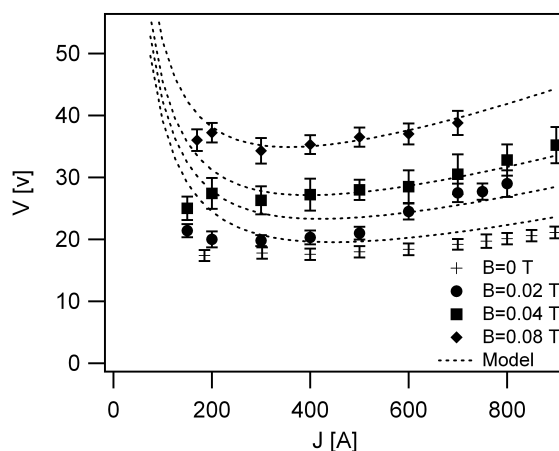

Figure 6. Voltage-Current characteristics for $\dot{m}$=20 mg/s. The dashed lines represent the semi-empirical voltage model presented in Eq. 4.

IV. Semi-Empirical Voltage Model

In order to analyze and understand the observed trends in voltage and efficiency we develop a semi-empirical voltage model.

The total voltage in MPDTs can be divided into three components as follows

$$V_{tot} = V_{res} + V_{emf} + V_E, \tag{3}$$

where V_{tot} is the total voltage between the anode and cathode. The first term on the right hand side (named V_{res}) represents the resistive component of the voltage and is affected by the total current, the plasma density and the plasma temperature. The second term (named V_{emf}) represents the back electromotive voltage and originates from the motion of the plasma through regions of finite magnetic field. The back electromotive voltage drop is affected by the total current, plasma velocity, applied magnetic field and mass flow rate. The third term (also named V_E) represents the voltage due to electrode losses in the anode and cathode sheaths. This mechanism was investigated in the past in self-field MPDT[15] and AF-MPDT.[16] In AF-MPDTs it was shown[15] that the anode voltage drop scales linearly with the applied magnetic field (B) and the applied current (J) and has a weak inverse dependence on the mass flow rate.
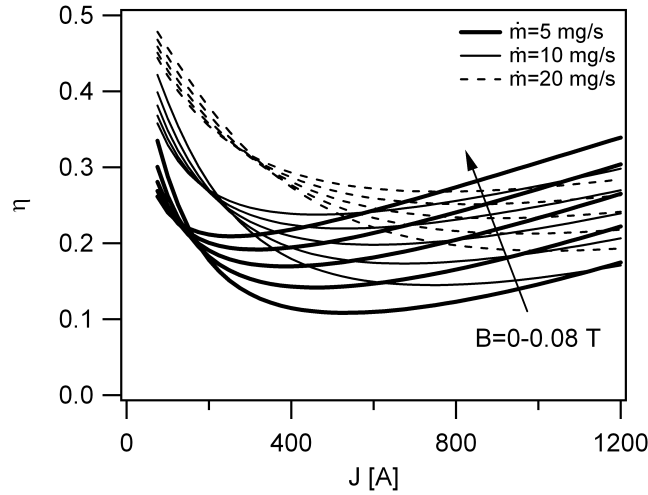
American Institute of Aeronautics and Astronautics

Figure 7. Efficiency Vs Current for various applied field and mass flow rate values.

	Observation
1	Both voltage (V) and efficiency (η) increase with applied magnetic field (B) for all values of current (J) and mass flow rate $(\dot{m})$.
2	Both voltage (V) and efficiency (η) are more sensitive to changes in current (J) and applied magnetic field (B) at low mass flow rate $(\dot{m})$ values.
3	Both voltage (V) and efficiency (η) exhibit a decreasing-increasing behavior with increasing current (J) for all applied magnetic field (B) and mass flow rate $(\dot{m})$ values. Each V-η curve has a minimum associated with it.
4	The minimum point moves to lower current (J) values with increasing applied field (B). The minimum point moves to higher current (J) values with decreasing mass flow rate $(\dot{m})$.

Table 1. Summary of observed trends in the voltage-current and efficiency-current curves

Based on previous studies and our present investigation, we constructed the following model for the total voltage,

$$V_{tot} = \frac{1}{J}\frac{\dot{m}\epsilon_i}{m_i} + \frac{1}{J}\frac{T^2}{2\dot{m}} + \phi_W + \frac{(C_{E1}J(C_{E2} + B_c) + C_{E3}B_c)}{\dot{m}^n}. \tag{4}$$

The first term represents the ionization voltage, which scales inversely with current. Since the ionization process in MPDTs is maintained via resistive heating, this term is part of the resistive heating voltage component. The plasma is assumed to be singly ionized with an ionization potential of $\epsilon_i = 5.391$ eV. The second term represents the back electromotive voltage component and is discussed below. The third term represents the electrodes' work function. Lithium-coated tungsten has a work function of approximately 2.5 eV[5] thus $\phi_W \simeq 5$ eV for the anode and cathode combined. The last term represents the electrodes' voltage fall and the heating part of the resistive voltage. The mathematical form of the last term and the four constants (C_{E1}, C_{E2}, C_{E3} and n) were found by finding the best fit of the the above expression to the measured voltage-current characteristics. This yielded the following values: $C_{E1} = 3.09 \times 10^{-4}$, $C_{E2} = 0.2$, $C_{E3} = 0.4636$ and $n = 0.5$. For simplicity we refer to the sum of all voltage components not including the back electromotive component as the non-useful voltage since it represents the sum of all power losses in thruster operation.

We employ Tikhonov's thrust expression (Eq. 2) in order to obtain a mathematical expression for the back electromotive voltage component (V_{emf}). All the three thrust components will therefore have an effect on the back electromotive voltage as can be seen in the expression below (Eq. 5).

American Institute of Aeronautics and Astronautics

$$V_{emf} = 1.28a_0^2\frac{\dot{m}}{J} + 0.16a_0(2r_a)B_a + 5\times10^{-3}(2r_a)^2\frac{B_a^2 J}{\dot{m}} + 2.736\times10^{-7}a_0 J + 3.42\times10^{-8}r_a\frac{B_a J^2}{\dot{m}} + 1.462\times10^{-14}\frac{J^3}{\dot{m}}$$
$$(5)$$

The first three terms represent the contribution of the gas dynamic and applied filed component to thrust. The last three components represent the contribution of the self-field component of thrust and are negligible at current values less than about 800 A.

Armed with the above mathematical expressions we can now analyze the observed trends in voltage and efficiency.

V.   Physical Interpretation

The first and probably most important observation made is the fact that the efficiency increases with increasing applied magnetic field. The reason for this behavior is found from Eqs. 4 and 5, where the efficiency is seen to be greater when the useful voltage component (V_{emf}) increases faster than the non-useful voltage ($V_{tot} - V_{emf}$) with the applied magnetic field. Since V_{emf} scales with B^2 while the non-useful voltage scales with B there is a general increase of the efficiency with B. From the mathematical form of the last term in Eq. 4 we can conclude that the heating and electrode sheath power losses are linear to the applied field, therefore the useful power increases faster than the non-useful power with increasing applied field.

From the semi-empirical model we conclude that the non-useful voltage component scales linearly with current (J) and applied magnetic field (B) and inversely with the square root of the mass flow rate ($\dot{m}$), as seen in Eq. 4. This result is important since it implies the following:

1. The non-useful voltage drop increases linearly with increasing current much like in self-field MPDTs.[15] This phenomenon is attributed to electrode sheath losses and is still not fully understood. In addition, the anode voltage drop was measured by Myers[16] in AF-MPDT and found to scale linearly with the current and applied magnetic field. This fact strengthens the assumption that the observed trend is due to electrode sheath power loss.

2. The non-useful voltage drop increases linearly with increasing applied magnetic field. Although Myers found the anode loss to scale with the applied field this phenomenon could not be attributed to electrode sheath effects since the sheath length is of the order of the Debye length which in MPDTs is 10^{-6} m while the electron gyro-radius is of the order of 10^{-4} m. Even though we cannot corroborate Myers' findings with the scale length analysis we can speculate that a different physical process, sensitive to magnetic field, is occurring. It is likely that the voltage drop discussed is resistive and is due to a decreasing conductivity with increasing applied magnetic field. With a decreasing conductivity the thruster will require operation with higher voltage fall in order to achieve the desired current. In order to verify this assumption one needs to estimate the conductivity using the generalized Ohm's law and measurements of the electric field and current density distributions - an elaborate and difficult process.

3. The conductivity change argument from above might also explain the inverse dependence on the mass flow rate. An increase in mass flow rate will increase the number density thus increasing the conductivity and reducing the voltage required to sustain the desired current.

We also observed that the increase in efficiency with increasing current and applied field is more sensitive when the mass flow rate is lower. This can be corrobrated with the fact that the back electromotive voltage scales with $(JB^2)/\dot{m}$ as seen in the third term in Eq. 5. Any changes in current or applied field will be greater for lower values of mass flow rate. This means that the enhancement of the efficiency by the applied magnetic field is greater when the mass flow rate is reduced.

The decreasing-increasing behavior of efficiency with current can be explained by considering the contribution of each thrust component to the back electromotive voltage. Each one of the three thrust components dominates thrust production in different current regimes. The thrust regime characterized by the lowest current values is the gas dynamic regime. This can be seen in Fig. 3 where at low current values the thrust consists mostly of the value of the non-current-dependent constant $1.6a_0\dot{m}$. The gas dynamic thrust component contributes the quantity $1.28a_0^2\dot{m}/J$ to the back electromotive voltage and therefore will decrease with increasing current. The reduction in this voltage component will contribute to the reduction in efficiency. When increasing the current even further the applied field component of thrust dominates the scaling of

thrust. This can be seen in Fig. 3 where at intermediate current values the thrust consists mostly of the value of the applied field component $(0.1(2r_a)B_aJ)$. The applied field thrust component contributes the quantity $5 \times 10^{-3}(2r_a)^2B_a^2J/\dot{m}$ to the back electromotive voltage thus scaling linearly with current much like the non-useful voltage. For this reason the efficiency curve flattens out and rises when the self-field component of thrust becomes larger. The following floor efficiency value can be calculated by taking the expression for efficiency at $J \to \infty$ and without considering the self field component of thrust,

$$\eta_{floor} = \left[1 + \frac{C_{E1}(B_c + C_{E2})\sqrt{\dot{m}}}{5 \times 10^{-3}(2r_a)^2B_a^2}\right]^{-1}. \tag{6}$$

We see that the floor efficiency increases with increasing applied magnetic field and decreasing with the mass flow rate. As mentioned above, further increase of efficiency with current is due to the effect of the self field thrust component on the back electromotive voltage. Since the latter scales with J^3 (which implies a vigorous increase with the total current) while the non-useful voltage scales with J the efficiency will rise with current.

The current value at which the efficiency reaches its minimum value can be found by solving the equation $\partial\eta(J)/\partial J = 0$ for J. Since the mathematical expression for the solution for J_{min} is too large it will not be quoted here but we explain the physical mechanisms controlling the value of J_{min}. As explained above the decreasing-increasing efficiency behavior is a result of magnitude interplay between the different thrust components at different current regimes. As seen in Eq. 5 high $\dot{m}$ will increase the first term ($\propto \dot{m}/J$) on the LHS, which corresponds to the gas dynamic thrust component, while decreasing the third term ($\propto J/\dot{m}$) which corresponds to the applied field thrust component. Therefore the recovery of the efficiency with current will be pushed to higher current values. On the other hand high applied magnetic field will not change the magnitude of the first term in Eq. 5 yet it will increase the second ($\propto B_a$) and third ($\propto B_a^2$) terms thus pushing the minimum point to lower current values.

Another explanation for the decreasing behavior of the voltage-current curves can be taken from work conducted on arcjets. Although geometrically similar, Arcjets and MPDTs operate at different current regimes. Since the arcjet operates at lower current than that of the MPDT (usually in the order of several to tens of Ampere) we can compare the voltage-current characteristics of the low current regime in the LiLFA to that of a typical arcjet. Indeed arcjets exhibit a similar decreasing trend of the voltage-current characteristics[17].[18] This behavior in arcjets is attributed to an increase in conductivity. As the current to the thruster is raised the propellant becomes hotter and more ionized. This increase in both temperature and ionization increases the conductivity which in turn reduces the voltage needed to sustain the arc. We may expect that a similar phenomenon occurs in the LiLFA at low current values (less than 200 A).

VI.   Conclusions

In order to shed light on the nature of scaling of AF-MPDT performance with applied magnetic field, we measured the voltage-current characteristics of an AF-MPDT at various applied magnetic field and mass flow rate values and employed a semi-empirical thrust model to obtain a mathematical expression for the thrust. Using both the voltage data and thrust formula we calculated the thruster's efficiency as it changes with changing current, applied magnetic field and mass flow rate. In addition, a semi-empirical expression for the voltage was derived in order to characterize the non-useful voltage.

We found that the efficiency increases with increasing applied magnetic field. This increase was found to be attributed to the contribution of the applied field to thrust thus increasing the back electromotive voltage. This increase was found to be greater than the increase of the non-useful voltage with the applied field.

The non-useful voltage was found to scale linearly with current and applied magnetic field and inversely with mass flow rate. We offered a speculation to this behavior by suggesting that the current dependence is due to sheath effects as in self-field MPDTs and the magnetic field behavior is due to a decrease in conductivity with an increasing applied magnetic field.

We also found that the efficiency-current curve has a decreasing-increasing behavior with a minimum point that is affected by both the applied magnetic field and mass flow rate. It was shown that the value of the current at this minimum point is higher when the mass flow rate increases and lower with a an increase in applied magnetic field. An expression for the floor value of efficiency was derived and it was shown that the minimum possible efficiency is larger for larger applied magnetic field.

These findings can be used to derive guidelines for AF-MPDT design, performance scaling and optimization.

Acknowledgments

References

[1] H. Maecker. Plasma jets in arcs in a process of self-induced magnetic compression. *Z. Phys.*, 141:198–216, 1955.

[2] R.G. Jahn. *Physics of Electric Propulsion*. McGraw-Hill, New York, 1968.

[3] E. Y. Choueiri. The scaling of thrust in self-field magnetoplasmadynamic thrusters. *Journal of Propulsion and Power*, 14(5):744–753, 1998.

[4] A.D. Kodys and E.Y. Choueiri. A critical review of the state-of-the-art in the performance of applied-field magneto-plasmadynamic thrusters. In *The 41st Joint Propulsion Conference (JPC), July 10-14, 2005, Tucson, AZ. AIAA-2005-4247*, 2005.

[5] J.E.Polk and T.J. Pivirotto. Alkali metal propellants for mpd thrusters. In *AIAA/NASA/OAI Conference on Advanced SEI Technologies, September 4-6, 1991, Cleaveland, OH. AIAA-91-3572*, 1991.

[6] V.P. Ageyev and V.G. Ostrovsky. High current stationary plasma accelerator of high power. In *The 23th International Electric Propulsion Conference (IEPC), 1993, Seattle, WA, IEPC-93-117*, 1993.

[7] V.B. Tikhonov, S.A. Semenikhin, J.R. Brophy, and J.E. Polk. Performance of 130kw mpd thruster with an external magnetic field and li as a propellant. In *The 25th International Electric Propulsion Conference (IEPC), Oct, 1997, Cleveland, Ohio, IEPC-97-117*, 1997.

[8] P.G. Mikellides and P.J. Turchi. A theoretical model for the thrust and voltage of applied-field mpd thrusters. The Ohio State University, Columbus, Ohio, USA, 1998.

[9] G. Popov, V. Kim, V.B. Tikhonov, and S. Semenikhin. The second quarterly report on the stage no 3 c,d of the contract on the research studies no nasw-4851 between riame mai and nasa. Technical report, 'RIAME', 'MAI', Moscow, Russia, April 1997.

[10] A.D. Kodys, G. Emsellem, L.D. Cassady, J.E. Polk, and E.Y. Choueiri. Lithium mass flow control for high power lorentz force accelerators. Princeton Univ., Princeton, NJ, USA, Jet Propulsion Lab, Pasadena, CA, 2001.

[11] Cassady L.D. *Lithium-Fed Arc Multichannel and Single-Channel Hollow Cathode: Experiment and Theory*. PhD thesis, Princeton Univ., 2006.

[12] G. Popov, V. Kim, V.B. Tikhonov, and S. Semenikhin. The first quarterly report on the stage no 3 a of the contract on the research studies no nasw-4851 between riame mai and nasa. Technical report, 'RIAME', 'MAI', Moscow, Russia, April 1996.

[13] G. Popov, V. Kim, V.B. Tikhonov, and S. Semenikhin. The second quarterly report on the stage no 3 b of the contract on the research studies no nasw-4851 between riame mai and nasa. Technical report, 'RIAME', 'MAI', Moscow, Russia, December 1996.

[14] G.A. Popov, V. Kim, V.B. Tikhonov, S.A. Semenikhin, and M.K. Tibrina. The third quarterly report on the milestones (a)(4) and (a)(5)(d) of sow of contract no 960938 between riame mai and jpl. Technical report.

[15] Kevin D. Diamant, Edgar Y.Choueiri, and R.G.Jahn. Spot mode transition and the anode fall of pulsed mpd thrusters. *Journal of propulsion and power*, 14(6):1036–1042, 1998.

[16] Roger M. Myers and George C. Soulas. Anode power deposition in applied-field mpd thrusters. In *The 28th Joint Propulsion Conference (JPC), July 6-8, 1992, Nashville, TN. AIAA-92-3463*, 1992.

[17] Terry L. Hardy and Francis M. Curran. Low power dc arcjet operation with hydrogen/nitrogen/ammonia mixtures. Technical report.

[18] B. Glocker, H.O. Schrade, and M. Auweter-Kurtz. Performance calculation of arc jet thrusters - the three channel model. In *The 23rd International Electric Propulsion Conference (IEPC), Sep, 1993, Seattle, WA, IEPC-93-187*, 1993.

American Institute of Aeronautics and Astronautics